



# Antiamoebic activity of synthetic tetrazoles against *Acanthamoeba castellanii* belonging to T4 genotype and effects of conjugation with silver nanoparticles

Areeba Anwar<sup>1</sup> · Yim Pei Yi<sup>1</sup> · Itrat Fatima<sup>2</sup> · Khalid Mohammed Khan<sup>2,3</sup> · Ruqaiyyah Siddiqui<sup>4</sup> · Naveed Ahmed Khan<sup>4</sup> · Ayaz Anwar<sup>1</sup>

Received: 28 January 2020 / Accepted: 15 April 2020  
© Springer-Verlag GmbH Germany, part of Springer Nature 2020

## Abstract

*Acanthamoeba* causes diseases such as *Acanthamoeba* keratitis (AK) which leads to permanent blindness and granulomatous *Acanthamoeba* encephalitis (GAE) where there is formation of granulomas in the brain. Current treatments such as chlorhexidine, diamidines, and azoles either exhibit undesirable side effects or require immediate and prolonged treatment for the drug to be effective or prevent relapse. Previously, antifungal drugs amphotericin B, nystatin, and fluconazole-conjugated silver with nanoparticles have shown significantly increased activity against *Acanthamoeba castellanii*. In this study, two functionally diverse tetrazoles were synthesized, namely 5-(3-4-dimethoxyphenyl)-1*H*-tetrazole and 1-(3-methoxyphenyl)-5-phenoxy-1*H*-tetrazole, denoted by T1 and T2 respectively. These compounds were evaluated for anti-*Acanthamoeba* effects at different concentrations ranging from 5 to 50 µM. Furthermore, these compounds were conjugated with silver nanoparticles (AgNPs) to enhance their efficacy. Particle size analysis showed that T1-AgNPs and T2-AgNPs had an average size of 52 and 70 nm respectively. After the successful synthesis and characterization of tetrazoles and tetrazole-conjugated AgNPs, they were subjected to anti-*Acanthamoeba* studies. Amoebicidal assay showed that at concentration 10 µM and above, T2 showed promising antiamoebic activities between the two compounds while encystation and excystation assays reveal that both T1 and T2 have inhibited differentiation activity against *Acanthamoeba castellanii*. Conjugation of T1 and T2 to AgNP also increased efficacy of tetrazoles as anti-*Acanthamoeba* agents. This may be due to the increased bioavailability as AgNP allows better delivery of treatment compounds to *A. castellanii*. Human cell cytotoxicity assay revealed that tetrazoles and AgNPs are significantly less toxic towards human cells compared with chlorhexidine which is known to cause undesirable side effects. Cytopathogenicity assay also revealed that T2 conjugated with AgNPs significantly reduced cytopathogenicity of *A. castellanii* compared with T2 alone, suggesting that T2-conjugated AgNP is an effective and safe anti-*Acanthamoeba* agent. The use of a synthetic azole compound conjugated with AgNPs can be an alternative strategy for drug development against *A. castellanii*. However, mechanistic and in vivo studies are needed to explore further translational values.

**Keywords** *Acanthamoeba* · Antiamoebic · Tetrazole · Nanoparticles

Section Editor: Julia Walochnik

✉ Ayaz Anwar  
ayazanwarkk@yahoo.com

<sup>1</sup> Department of Biological Sciences, School of Science and Technology, Sunway University, 47500 Subang Jaya, Selangor, Malaysia

<sup>2</sup> H. E. J. Research Institute of Chemistry, International Center for Chemical and Biological Sciences, University of Karachi, Karachi 75270, Pakistan

<sup>3</sup> Department of Clinical Pharmacy, Institute for Research and Medical Consultations (IRMC), Imam Abdulrahman Bin Faisal University, Dammam 31441, Saudi Arabia

<sup>4</sup> Department of Biology, Chemistry and Environmental Sciences, College of Arts and Sciences, American University of Sharjah, Sharjah 26666, United Arab Emirates

## Introduction

*Acanthamoeba*, an opportunistic pathogen, is commonly found in soil and water (Köhler et al. 2016). A blinding infection of the eye known as *Acanthamoeba* keratitis (AK) is caused by the invasion of *Acanthamoeba* in the eye where it causes chronic ulceration of the cornea which often leads to permanent sight damage. AK usually occurs in contact lens wearing individuals where the malpractice of contact lenses is the main cause, such as wearing contact lenses while swimming activities (Siddiqui and Khan 2012). Another human disease caused by *Acanthamoeba* is granulomatous amoebic encephalitis (GAE), where the pathogen invades the central nervous system (CNS) and causes the formation of granulomas (Siddiqui and Khan 2012). GAE is known to be an opportunistic infection as it occurs mainly in immunocompromised individuals (Slater et al. 1994). This disease is rare but highly fatal as statistics show 95% of recorded patients die even when they are given different antimicrobial treatments (Kulsoom et al. 2014). Besides these two infections, *Acanthamoeba* also causes the lung, kidney, and skin to be compromised by the pathogen, where trophozoites and cysts usually surround the walls of blood vessels. *Acanthamoeba* may feed on skin tissue and cause severe skin lesions in immunocompromised patients as well (Schuster and Visvesvara 2004).

*Acanthamoeba* can exist as a free-living unicellular microorganism in nature or as a parasite inside a host. *Acanthamoeba* is known to feed on bacteria in their environments and support the growth of several other pathogens, such as *Mycobacterium*, *Chlamydia*, and certain viruses (Khan 2006). The pathogen undergoes asexual reproduction by dividing through binary fission (Band and Mohrlok 1973). There are two phases in the life cycle of *Acanthamoeba*: growth phase trophozoites and cellular differentiation to form cysts. The two types of cellular differentiation are known as encystment and excystment (Weisman 1976). Excystment leads to *Acanthamoeba* trophozoites from cysts which is the active form and is described as having protruding spine-like structure known as acanthopodia which are important for movement, engulfing bacteria, and surface adhesion. Encystment, on the other hand, leads to *Acanthamoeba* cysts from trophozoites, which are the resistant form of the pathogen, when it is subjected to a harsh environment such as starvation, dryness, and extreme temperatures (Khunkitti et al. 1998). Cysts are described as double walled with a wrinkled ectocyst (outer layer) and an endocyst (inner layer) which varies in shape. At the site of contact between the ectocyst and endocyst, pores covered by small lids (operculum) are present (Siddiqui and Khan 2012). These cyst walls are made up of polysaccharides of glucose and galactose; hence, polysaccharides biosynthesis pathway is considered as an important target for the development of treatments against

*Acanthamoeba* cysts (Garajová et al. 2019; Anwar et al. 2019).

The current recommended treatment for AK is biguanide such as chlorhexidine together with a diamidine and added antibiotics if the bacterial infection was involved (Lorenzo-Morales et al. 2015). Chlorhexidine releases a cation that interacts with the cell membrane, hence increasing cell permeability and ultimately leading to cell death through leakage of ions and cytoplasmic disruption (Sharma et al. 2013). Although chlorhexidine is effective against *A. castellanii*, immediate and aggressive treatment with the biguanide is needed to make the treatment effective (Lamb et al. 2015). Chlorhexidine also exhibits undesirable effects when treated against AK such as mature cataracts and iris atrophy (Aqeel et al. 2016). Other anti-protozoa drug currently used are azoles such as metronidazole, which is notably effective against amoebic infections in the human gastrointestinal tracts caused by *Entamoeba histolyca* (Cano et al. 2014). However, the issue of metronidazole-resistant protozoa has also been brought into light and the drug is known to cause undesirable side effects such as headaches and dry mouth and is potentially toxic (Bendensky et al. 2002). There are reports of using a mixture of metronidazole, chlorhexidine, and neomycin sulfate that led to rapid resolution of inflammation in AK (Xuguang et al. 2003). Other than metronidazole, voriconazole is also found to be effective in treatment of AK; however, prolonged treatment with the drug was required to prevent relapse (Tu et al. 2010). Next, ketoconazole was found to be effective against a brain abscess caused by *Acanthamoeba* when treated together with a mixture of antibiotics (Nampoothiri et al. 2018). However, ketoconazole has previously shown high hepatotoxicity and endocrine dysregulation, which led to the ban of the azole in the Australian and European markets as well as strict regulations in America (Gupta and Lyons 2015). Previously, several triazole antifungal agents were tested against *Acanthamoeba castellanii* and *Acanthamoeba polyphaga* by inhibiting the sterol 14-demethylase (CYP51) (Lamb et al. 2015). It was found that *Acanthamoeba* is more related to algae and plants than mammalian ancestries; therefore, existing antifungal azoles were not very effective anti-*Acanthamoeba* agents due to the low sequence identity of *Acanthamoeba* and fungal CYP51 as shown by NCBI-BLASTP (Lamb et al. 2015).

Besides known azole drugs, synthetic azoles are also of widespread interest for drug development against numerous microbes. Tetrazoles are five-membered aromatic ring compounds with four nitrogen and one carbon atom. This planar structure makes the compound electron rich and allows the compound to form weak bonds with enzymes or biological receptors (Lingling et al. 2013). This characteristic also allows tetrazoles to interact and stabilize functional molecules that were formed through combination of multiple small molecules, showing many potentials in the pharmaceutical industry

(Dai et al. 2015). Besides, tetrazoyl fragments have been described as the non-toxic and non-metabolized analogues of carboxylic and cis-amide groups (Dai et al. 2015). Certain derivatives of tetrazoles have also shown strong antifungal activities through inhibition of ergosterol synthesis such as tetrazole derivatives which contain hydrazone and thiazoline portion shows high efficacy in inhibiting certain *Candida*, *Aspergillus*, and *Fusarium* species (Łukowska-Chojnacka et al. 2016). Several types of synthetic chromone-tetrazoles have also shown to be effective against *Entamoeba histolytica*, the causative agent of amoebic diarrhea and dysentery (Cano et al. 2014). Among membrane-acting agents, alkylphosphocholines such as miltefosine have been found to be effective against AK and GAE (Tavassoli et al. 2018; Barisani-Asenbauer et al. 2012; Webster et al. 2012). Furthermore, synthetic analogues of alkylphosphocholines have also been reported to exhibit potent antiamoebic effects against *Acanthamoeba* spp. (Timko et al. 2015; Garajová et al. 2014).

Nanoparticles may be the solution to multidrug-resistant pathogens as they have shown to increase the efficacy of compounds against various microbes (Egger et al. 2009). Researchers are interested in silver nanoparticles because silver was used as an antimicrobial agent against bacteria (Bello-Vieda et al. 2018). Besides that, conjugation of natural products, plant extracts, and contact lens solutions to silver nanoparticles have been shown to increase the in vitro effectivity of their payloads against *Acanthamoeba* spp. (Anwar et al. 2020; Padzik et al. 2018; Padzik et al. 2019). The mechanism of silver nanoparticles against microbes is still not fully grasped, but several mechanisms have been proposed. It is said that silver nanoparticles alter cell wall and cell membrane which in turn increases cell permeability (Bello-Vieda et al. 2018). Previously, antifungal drugs amphotericin B, nystatin, and fluconazole conjugated silver nanoparticles showed significantly increased activity against *Acanthamoeba castellanii* (Anwar et al. 2018). Developing a novel tetrazole silver nanoparticle with increased efficacy compared with the respective tetrazole alone against the human pathogen *Acanthamoeba* is the overall aim of this current study. In this study, we tested the antiamoebic properties of two novel synthetic tetrazoles against *A. castellanii* belonging to the T4 genotype and the effects of silver nanoparticles conjugation on the efficacy of these compounds.

## Materials and methods

### Chemicals

Different aromatic nitriles were purchased from different chemical suppliers including Alfa-Aesar, Merck, Sigma-Aldrich, and TCI. Silver nitrate ( $\text{AgNO}_3$ ) and sodium

borohydride ( $\text{NaBH}_4$ ) was obtained from Merck, RPMI-1640 was obtained from Gibco, and absolute DMSO was obtained from Thermo Scientific.

### *Acanthamoeba castellanii* cultures

A clinical isolate obtained in 1984 from a keratitis patient from India, *A. castellanii* of T4 genotype (ATCC 50492) was purchased from American Tissue Culture Collection (ATCC). The Amoeba cells were cultured in 10 ml of PYG medium consisting of 0.75% yeast extract, 0.75% protease peptone, and 1.5% glucose in T-75  $\text{cm}^2$  culture flasks (Aqeel et al. 2016).

### Henrietta Lacks cell cultures

HeLa cells (CCL-2) were obtained from American Tissue Culture Collection (ATCC). The cells were cultured in RPMI-1640 supplemented with 1% (2 mM) L-glutamine, 1% penicillin-streptomycin, 10% fetal bovine serum, and 1% minimal essential media nonessential amino acid (MEM NEAA). The cells were incubated in a  $\text{CO}_2$  incubator at 37 °C and 95% humidity. Two milliliters (0.25%) of trypsin was used to detach the cells which enabled the inoculation of cells into 96-well plates.

### Synthesis and characterization of T1 and T2

The tetrazoles tested in this study are 5-(3-4-dimethoxyphenyl)-1*H*-tetrazole and 1-(3-methoxyphenyl)-5-phenoxy-1*H*-tetrazole, represented by T1 and T2 respectively (Fig. 1).

T1 and T2 were synthesized by click reaction of aromatic nitriles with sodium azide in the presence of ammonium chloride to afford T1 and T2 as given in Scheme 1 (Fatima et al. 2018).

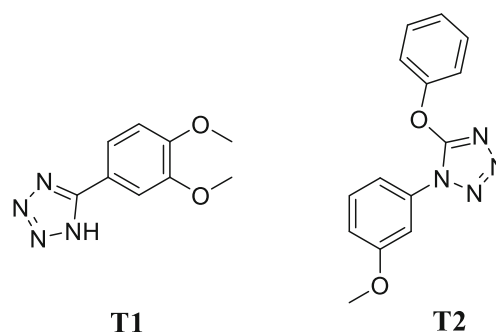
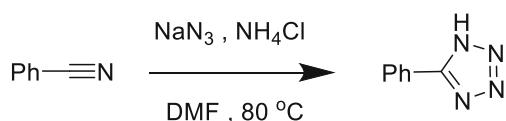


**Fig. 1** The chemical structures of 5-(3-4-dimethoxyphenyl)-1*H*-tetrazole (T1) and 1-(3-methoxyphenyl)-5-phenoxy-1*H*-tetrazole (T2)



**Scheme 1** Synthesis of Tetrazoles T1 and T2 (Fatima et al. 2018)

## Characterization of T1 and T2

### 5-(3',4'-Dimethoxyphenyl)-1H-tetrazole (T1)

Yield: 88%; m.p. 207–208 °C;  $^1\text{H-NMR}$ : (300 MHz, DMSO- $d_6$ ):  $\delta_H$  16.62 (s, NH), 7.63 (s, 1H, H-2'), 7.62 (d, 1H,  $J_{6',5'} = 8.4$  Hz, H-6'), 7.18 (d, 1H,  $J_{5',6'} = 8.4$  Hz, H-5'), 3.84 (s, 3H, 3'-OCH<sub>3</sub>), 3.83 (s, 3H, 4'-OCH<sub>3</sub>);  $^{13}\text{C-NMR}$  (100 MHz, DMSO- $d_6$ ):  $\delta_c$  151.1 (C-3'), 149.1 (C-4'), 120.1 (C-6'), 112.1 (C-2'), 110.0 (C-5'), 55.7 (4'-OCH<sub>3</sub>), 55.6 (3'-OCH<sub>3</sub>); IR (KBr,  $\text{cm}^{-1}$ ): 3477 (N-H), 1609 (C=N), 1144 (C-O); EI-MS:  $m/z$  (rel. abund. %), 206 [ $\text{M}^+$ ] (1), 191 (4), 182 (100), 152 (50), 136 (90); HREI-MS:  $m/z$  calcd for  $\text{C}_9\text{H}_{10}\text{N}_4\text{O}_2$  [ $\text{M}^+$ ] 206.0804; found 206.0791.

### Methyl2-[(1-phenyl-1H-1,2,3,4-tetrazol-5-yl)oxy]phenyl ether (T2)

Yield: 84%; m.p. 249–251 °C;  $^1\text{H-NMR}$ : (300 MHz, DMSO- $d_6$ ):  $\delta_H$  7.84 (d, 2H,  $J_{2',3'} = J_{6',5'} = 7.5$  Hz, H-2',6'), 7.68 (m, 3H, H-3',4',5'), 7.42 (dd, 1H,  $J_{4'',5''} = 9$ , Hz  $J_{4'',3''} = 8.4$  Hz, H-4''), 7.13 (m, 1H, H-5''), 7.07 (d, 1H,  $J_{6'',5''} = 7.8$  Hz, H-6''), 6.93 (d, 1H,  $J_{3'',4''} = 8.1$  Hz, H-3''), EI-MS:  $m/z$  (rel. abund. %), 268 ( $\text{M}^+$ , 4), 238 (36), 225 (4), 117 (100); HREI-MS:  $m/z$  calcd for  $\text{C}_{14}\text{H}_{12}\text{O}_2\text{N}_4$  [ $\text{M}^+$ ] 268.0960; found 268.0941.

## Synthesis of tetrazole-conjugated AgNPs

Tetrazoles were weighed and dissolved in absolute DMSO to prepare 10-mM stocks. The 10-mM stocks of the tetrazoles were diluted with sterile water to prepare 0.5-mM and 0.1-mM stocks which was used to plate concentrations 5  $\mu\text{M}$ , 10  $\mu\text{M}$ , 25  $\mu\text{M}$ , and 50  $\mu\text{M}$  in each assay. Synthesis of tetrazole-conjugated AgNPs was done by adding 2 ml of 0.1 mM tetrazole to 2 ml of 0.1 mM silver nitrate(aq) solution and mixed on a magnetic stirrer. Sodium borohydride (4 mM, 20  $\mu\text{l}$ ) was added to reduce the silver ions to enable conjugation of tetrazole to AgNP (Anwar et al. 2018). The successful formation was indicated by the color change of the mixture from colorless to yellow. Further analysis such as UV-Vis spectrophotometry and FT-IR spectroscopy was done to confirm the formation and stabilization of tetrazole-conjugated AgNPs.

## Amoebicidal assays

The antiamoebic properties of tetrazoles alone and tetrazole-conjugated AgNPs were tested in duplicates for this assay, as

described by Sissons et al. (2006). In 24-well plates,  $5 \times 10^5$  *A. castellanii* trophozoites were treated with 5  $\mu\text{M}$ , 10  $\mu\text{M}$ , 25  $\mu\text{M}$ , and 50  $\mu\text{M}$  of T1 and T2 respectively as well as 5  $\mu\text{M}$  and 10  $\mu\text{M}$  of tetrazole-conjugated AgNPs and AgNPs alone in RPMI-1640. Chlorhexidine served as the positive controls and RPMI-1640 alone as the negative control. Appropriate amounts of DMSO and water were also plated as solvent controls. After a 24-h incubation period at 30 °C, a trypan blue exclusion assay was carried out to calculate the estimated average well count for each duplicate.

## Encystation assays

In 24-well plates,  $5 \times 10^5$  *A. castellanii* trophozoites were treated with 5  $\mu\text{M}$ , 10  $\mu\text{M}$ , 25  $\mu\text{M}$ , and 50  $\mu\text{M}$  of T1 and T2 respectively as well as 5  $\mu\text{M}$  and 10  $\mu\text{M}$  of tetrazole-conjugated AgNPs and AgNPs alone. All treatment was done in encystation medium comprised of 5 mM  $\text{MgCl}_2$  and 10% glucose. Chlorhexidine served as the positive controls and PBS containing an encystation medium served as the negative control. Appropriate amounts of DMSO and water were also plated as solvent controls. After a 96-h incubation period at 30 °C, 0.1% SDS was added to dissolve trophozoites to enable the counting of cysts using a hemocytometer.

## Excystation assay

Preparation of cysts was done few weeks prior to this experiment by plating healthy *A. castellanii* trophozoites on non-nutrient agar plates for at least 14 days before it was scraped and collected.  $1 \times 10^5$  cysts were treated with 5  $\mu\text{M}$ , 10  $\mu\text{M}$ , 25  $\mu\text{M}$ , and 50  $\mu\text{M}$  of T1 and T2 respectively as well as 5  $\mu\text{M}$  and 10  $\mu\text{M}$  of tetrazole-conjugated AgNPs and AgNPs alone in PYG. Chlorhexidine served as the positive controls and PYG alone as the negative control. Appropriate amounts of DMSO and water were also plated as solvent controls. After a 96-h incubation period at 30 °C, a trypan blue exclusion assay was carried out to calculate the estimated average well count (trophozoites only) for each duplicate.

## Host cell cytotoxicity assays

In 96-well plates, HeLa cells were treated with 5  $\mu\text{M}$ , 10  $\mu\text{M}$ , 25  $\mu\text{M}$ , and 50  $\mu\text{M}$  of T1 and T2 respectively as well as 5  $\mu\text{M}$  and 10  $\mu\text{M}$  of tetrazole-conjugated AgNPs and AgNPs alone in RPMI-1640. Chlorhexidine served as the positive treatment and RPMI-1640 alone as the negative treatment. The positive control and negative control were achieved in quadruplicates by treating HeLa cells with 1% Triton X-100 (100% cell death) and incubating in RPMI-1640 alone respectively. After the 24-h incubation period, the supernatant of each well was transferred to microcentrifuge tubes. Lactate dehydrogenase enzyme (LDH) assay was carried out using a cytotoxicity



detection kit to measure absorbance reading at 490 nm. % cytotoxicity was calculated as (sample absorbance-negative control absorbance)/(positive control absorbance-negative control absorbance)  $\times$  100 (Aqeel et al. 2015).

### Host cell cytopathogenicity assays

In 24-well plates,  $5 \times 10^5$  *A. castellanii* trophozoites were treated with 5  $\mu$ M, 10  $\mu$ M, 25  $\mu$ M, and 50  $\mu$ M of T1 and T2 respectively as well as 5  $\mu$ M and 10  $\mu$ M of tetrazole-conjugated AgNPs and AgNPs alone in RPMI-1640. Chlorhexidine served as the positive treatment and RPMI-1640 alone as the negative treatment. After a 2-h incubation period, the treated trophozoites were centrifuged at 3000 rpm for 10 min and resuspended in 200  $\mu$ l RPMI-1640 to retrieve viable trophozoites. The treated trophozoites were used to treat HeLa cells in 96-well plates at 37 °C for 24 h. The positive control and negative control were achieved in quadruplicates by treating HeLa cells with 1% Triton X-100 (100% cell death) and incubating in RPMI-1640 alone respectively. After the 24-h incubation period, the supernatant of each well was transferred to microcentrifuge tubes. Lactate dehydrogenase enzyme (LDH) assay was carried out using a cytotoxicity detection kit to measure absorbance reading at 490 nm. % cytopathogenicity was calculated as (sample absorbance-negative control absorbance)/(positive control absorbance-negative control absorbance)  $\times$  100 (Aqeel et al. 2015).

### Statistical analysis

The results were shown as mean  $\pm$  standard error of the three experiments performed in duplicates for each compound. The significance of the differences between the averages of negative and sample well counts were determined by using a two-sample *t* test with a two-tailed distribution, done on Microsoft Excel.

## Results

### Analyzing the conjugation of tetrazoles with silver nanoparticles with UV-Vis spectrophotometry, dynamic light-scattering, and Fourier-transform infrared spectroscopy

To ensure the conjugation of T1 and T2 to silver nanoparticles, the synthesized compounds were analyzed using UV-Vis spectrophotometry. From Fig. 2, the maximum absorption for T1-AgNP and T2-AgNP was observed at 417 nm and 398 nm respectively. Both maximum absorptions were within the range of the peak shown by AgNP which was expected to have a surface plasmon resonance (SPR) band at the range of 350 nm to 450 nm (Anwar et al. 2018). This shows that both tetrazoles have been successfully conjugated to the AgNP.

DLS confirmed that the average size of nanoconjugates to be 52 and 70 nm. Figure 2b shows the T1-conjugated nanoparticles while Fig. 2c shows T2-conjugated nanoparticles as compared with compounds alone. Both FT-IR spectra show that the stabilization of nanoparticles was achieved by nitrogen of the tetrazole rings.

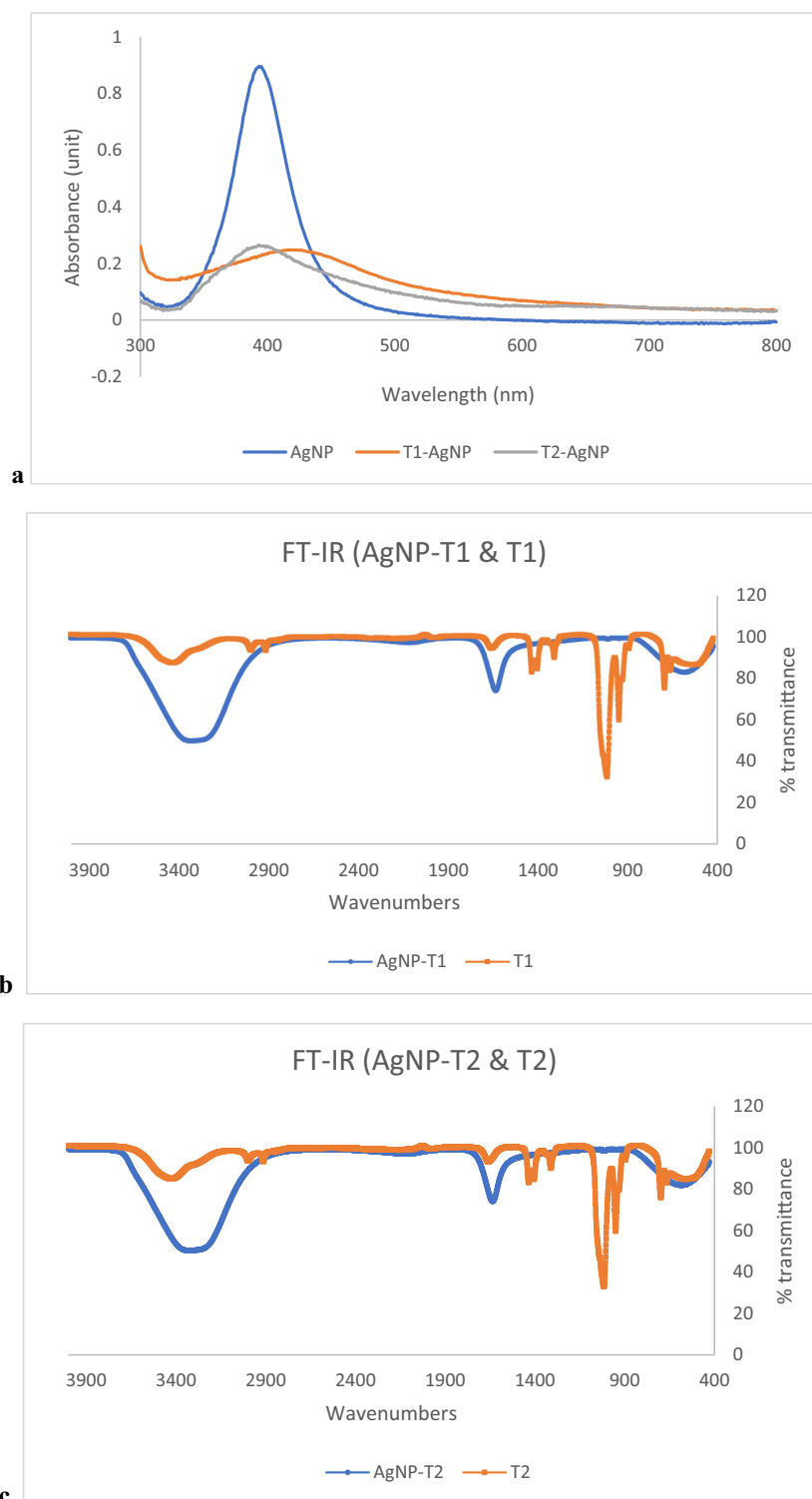
### Increased antiamoebic activity was observed in tetrazole-conjugated AgNPs compared with tetrazoles alone

To determine the antiamoebic activity of tetrazoles alone and conjugated with AgNPs against *A. castellanii*, amoebicidal assays were carried out for each drug in duplicates for three times. Figure 3a shows the antiamoebic effect of T1 and T2 for all concentrations as compared with the negative control ( $5 \times 10^5$  trophozoites in RPMI-1640 alone). T1 did not exhibit significant amoebicidal activity while T2 showed significant and dose-dependent antiamoebic activity from 10 to 50  $\mu$ M ( $*P < 0.05$ ). The antiamoebic effect increased significantly when concentration was increased from 10 to 25  $\mu$ M. IC<sub>50</sub> of T2 was estimated to be within 10  $\mu$ M to 25  $\mu$ M. Figure 3b shows that both tetrazole-conjugated AgNP had higher antiamoebic activity compared with respective tetrazoles alone. However, only 10  $\mu$ M T2-AgNP showed statistical significance when compared with negative control ( $5 \times 10^5$  trophozoites in RPMI-1640 alone), solvent control (AgNPs alone), and T2 alone ( $**P < 0.01$ ). Figure 3b shows that the T2-AgNPs showed a 50% reduction in the viability of *A. castellanii* at 10  $\mu$ M which corresponds to the IC<sub>50</sub>. This indicates that the conjugation of T2 to AgNP significantly increased the antiamoebic properties of T2 at 10  $\mu$ M.

### Encystation of *A. castellanii* was inhibited with tetrazoles and nanoparticles

To determine the ability of the tetrazoles and AgNP-conjugated tetrazoles to prevent *A. castellanii* from converting from trophozoites to its dormant and more resistant form, cysts, encystation assay was carried out in duplicates for three times. Figure 4a shows that overall inhibition of encystation was higher for T2 compared with T1. Inhibition of encystation in T1 showed statistical difference for 10  $\mu$ M ( $**P < 0.01$ ), 25  $\mu$ M ( $*P < 0.05$ ), and 50  $\mu$ M ( $***P < 0.001$ ). Inhibition of encystation of T2 showed higher significance for all concentrations ( $***P < 0.001$ ). From Fig. 4b, it can be observed that both T1-AgNP and T2-AgNP exhibited higher inhibition activity compared with respective tetrazoles. However, only T1-AgNP showed statistical significance as compared with the negative control ( $5 \times 10^5$  trophozoites in encystation medium), solvent control (AgNPs alone), and T1 alone ( $**P < 0.01$ ). This indicates that the conjugation of T1 to AgNP significantly increased the inhibition of encystation at 5  $\mu$ M.

**Fig. 2** **a** The UV-Vis spectra for AgNP, T1-AgNP, and T2-AgNP. Maximum absorptions observed for AgNP, T1-AgNP, and T2-AgNP were at 393 nm, 417 nm, and 398 nm respectively. **b** and **c** Comparative FT-IR spectra for T1-AgNP and T2-AgNP with T1 and T2 respectively

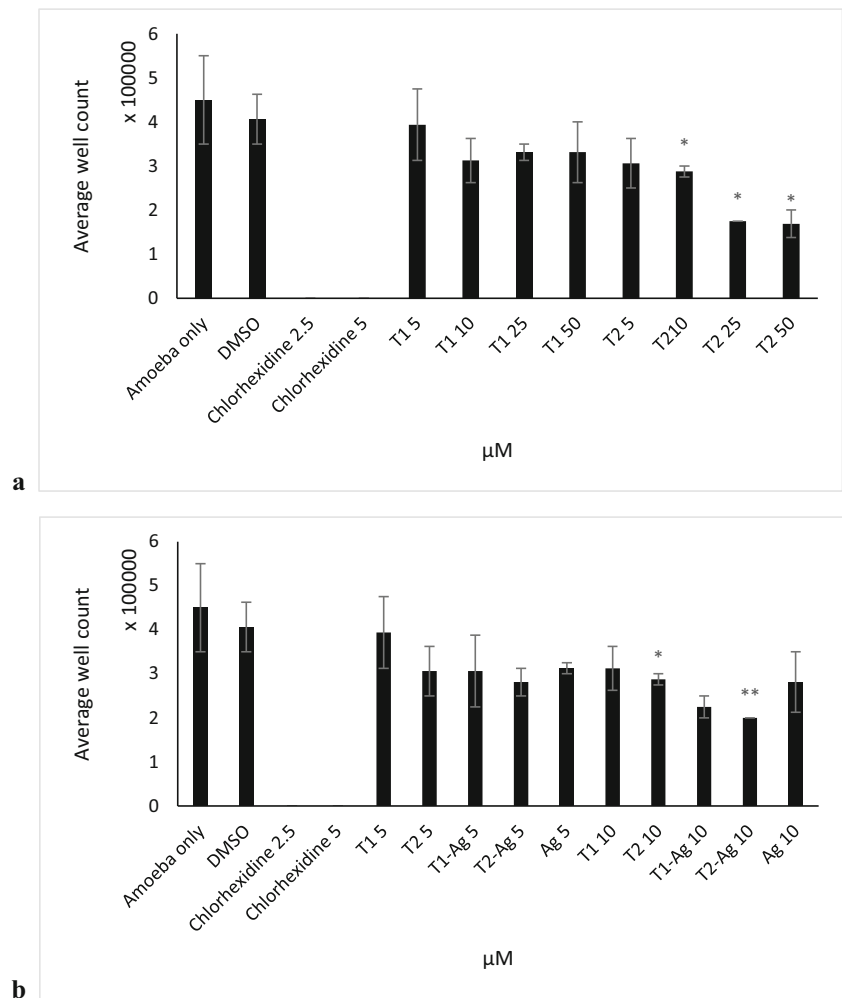


### Excystation of *A. castellanii* was inhibited with tetrazoles and nanoparticles

To determine the ability of tetrazoles alone and conjugated to AgNP to prevent *A. castellanii* cyst from reverting back to

trophozoites, excystation assay was carried out in duplicates for three times. Figure 5a shows that both T1 and T2 have shown significant inhibition activities compared with the negative control (cyst alone) (\*\* $P < 0.01$ ). However, activities of T1 at 25  $\mu$ M and 50  $\mu$ M, as well as T2 at 50  $\mu$ M, showed

**Fig. 3** **a** Antiamoebic activity of T1 and T2 alone. **b** Antiamoebic activity of T1 and T2 conjugated with a silver nanoparticle. The assay was carried out by incubating each compound at concentrations 5  $\mu$ M, 10  $\mu$ M, 25  $\mu$ M, and 50  $\mu$ M with  $5 \times 10^5$  trophozoites in RPMI-1640 at 30 °C for 24 h. Trypan blue exclusion assay was used to estimate the number of viable cells in each well and the average well count was calculated for each duplicate



statistical significance when compared with solvent control (0.025% DMSO (\* $P < 0.05$ )). At 25  $\mu$ M, T1 shows higher effectiveness compared with T2. However, the effectiveness of T1 plateaued when concentration was increased to 50  $\mu$ M. IC<sub>50</sub> of T1 is estimated to be between 5  $\mu$ M and 10  $\mu$ M. From Fig. 5b, both tetrazole-conjugated AgNPs are shown to be slightly more effective compared with respective tetrazoles alone at concentration 5  $\mu$ M. However, only 5  $\mu$ M T2-AgNP showed statistical significance when compared with the negative control ( $1 \times 10^5$  cysts), solvent control (AgNPs alone), and T2 alone (\* $P < 0.05$ ). This indicates that the conjugation of T2 to AgNPs significantly increases the inhibition of excystation at 5  $\mu$ M.

#### Tetrazole-conjugated AgNPs and tetrazoles alone exhibited low human cell cytotoxicity

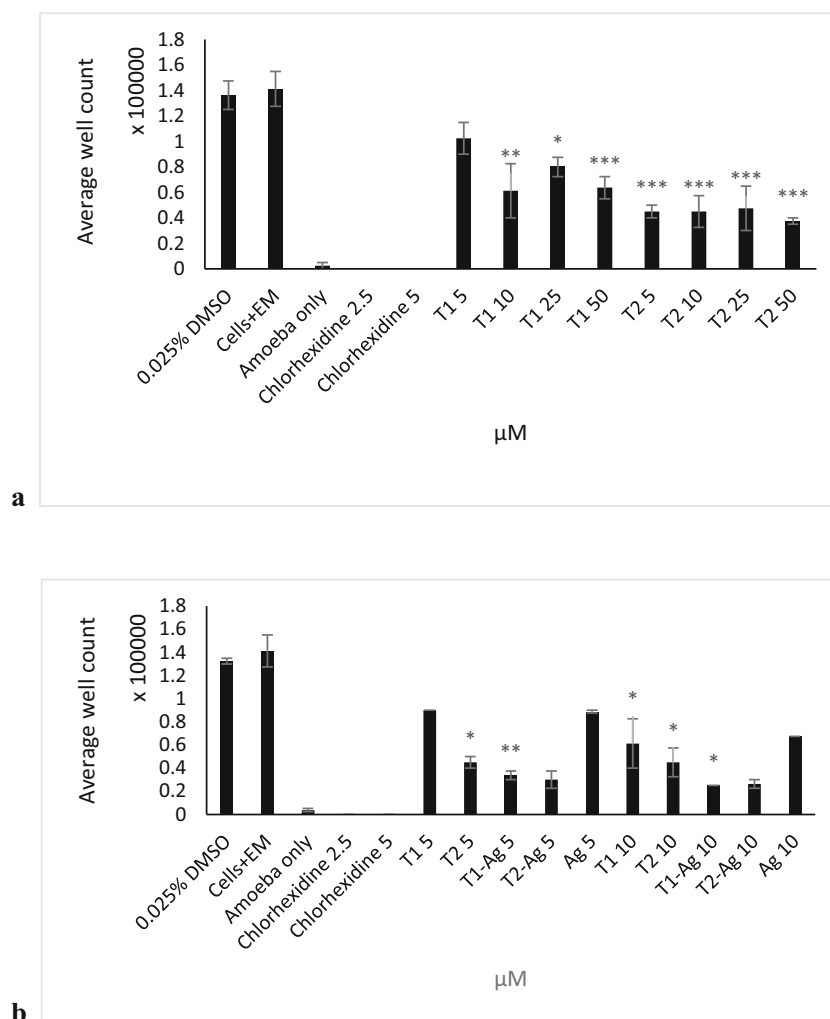
To evaluate the cell-damaging effects of tetrazole-conjugated AgNPs and tetrazoles alone on human HeLa cells, cytotoxicity assay was carried out in duplicates. From Fig. 6, T1-conjugated

AgNPs exhibited the highest % cytotoxicity (18.6% and 14.8%) among all samples. However, all samples, including T1-conjugated AgNPs, showed lower % cytotoxicity compared with chlorhexidine (39% cytotoxicity) at 10  $\mu$ M. Solvents used to prepare tetrazoles and NPs showed lower % cytotoxicity compared with Triton X and chlorhexidine as well.

#### Tetrazole-conjugated AgNPs significantly decreased cytopathogenicity of *A. castellanii*

To evaluate the *A. castellanii*-mediated cytotoxicity against HeLa cells after being treated with tetrazole-conjugated AgNPs and tetrazoles alone, cytopathogenicity assay was carried out in duplicates. Figure 7 shows that both T1 and T2 alone significantly decreased % cytopathogenicity of *A. castellanii* (\* $P < 0.05$ ) compared with untreated *A. castellanii* (89%) only. T2-conjugated AgNPs exhibited significantly lower % cytopathogenicity compared with T2 alone (\* $P < 0.05$ ).

**Fig. 4** **a** The effects of T1 and T2 on the encystation of *A. castellanii*. **b** The effects of T1-AgNP and T2-AgNP on the encystation of *A. castellanii* compared with T1 and T2 alone as well as AgNPs alone. The assay was carried out by incubating each compound with  $5 \times 10^5$  trophozoites in PBS at 30 °C for 96 h. A total of 0.1% SDS was used to dissolve remaining trophozoites and the cysts were counted to calculate average well count for each duplicate. Statistical significance of the inhibition effects was determined using two-sample *t* test with two-tailed distribution, done on Microsoft Excel



## Discussion

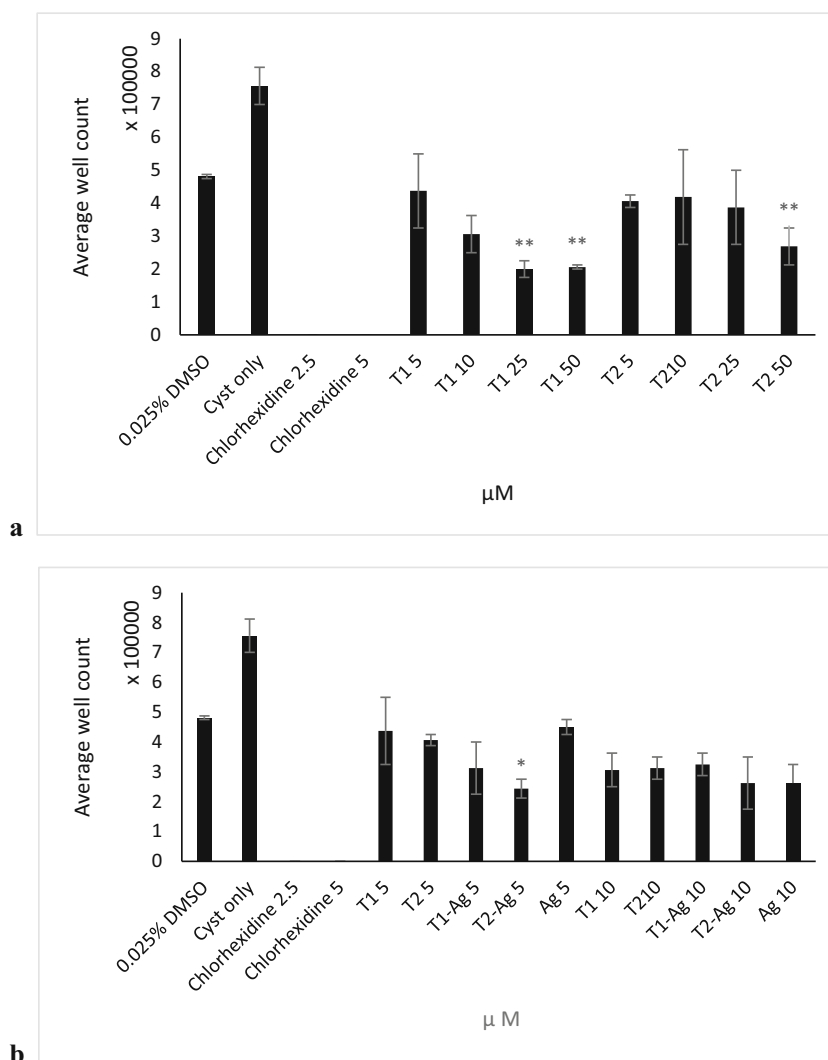
The major problems in GAE treatment are the formation of cysts and difficulty of drug delivery through the blood-brain barrier (BBB) due to the tight junctions; therefore, it is important to research for a formulation that can better penetrate the BBB (Anwar et al. 2018). Currently, one of the biggest challenges in research is delivering a drug to the site of treatment and release the drug at a specific rate to ensure maximum potency; thus, researchers are interested in developing efficient drug delivery systems (Kim et al. 2009). Drugs are usually low in potency due to low solubility which leads to aggregation, as well as short half-lives which causes the drug to degrade before reaching the target site (Parveen et al. 2012). Nanoparticles have much to offer in drug delivery as they allow the transport of drugs to specific target sites, sustained release of drugs, and are highly stable (Parveen et al. 2012). Metal nanoparticles such as AgNP were described to increase bioavailability and efficacy by reducing the size and shape of

conjugated compounds and functioning as a drug carrier (Zazo et al. 2016).

Azoles are usually used as antifungal agents with a mode of actions such as ergosterol and CYP51 inhibition (Chopra and Khuller 1983; Hitchcock et al. 1990). Azoles were used in treating *Acanthamoeba* as ergosterol was found to be present on the membrane of the pathogen (Cabello-Vílchez et al. 2014). A study was also done by Lamb et al. (2015), where several antifungal agents such as fluconazole, itraconazole, and voriconazole were used to inhibit CYP51 of *Acanthamoeba*. However, treatment was not effective as *Acanthamoeba* and fungal CYP51 have low sequence identity as shown by NCBI-BLAST (Lamb et al. 2015). Existing treatments are also not effective against all strains of *Acanthamoeba*; therefore, it is crucial to perform mechanistically and in vivo studies to better understand the receptors and molecules that play a role in the pathogenesis of *Acanthamoeba* (Lorenzo-Morales et al. 2015).



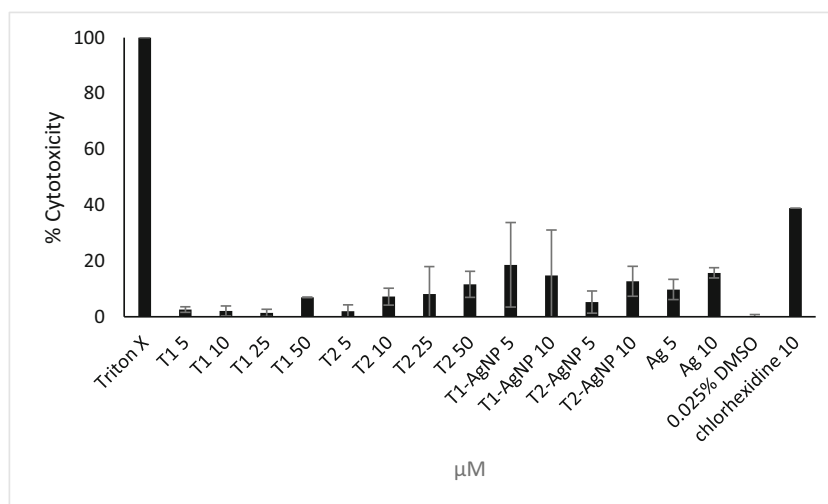
**Fig. 5** **a** The effectiveness of T1 and T2 on inhibiting the excystation of *A. castellanii*. **b** The effectiveness of T1-AgNP and T2-AgNP on inhibiting the excystation of *A. castellanii* compared with T1 and T2 alone. The assay was carried out by incubating each compound with  $5 \times 10^5$  cysts in PYG at 30 °C for 96 h. The viable trophozoites were counted with trypan blue exclusion assay and the average well count was calculated for each duplicate



As UV-Vis results (Fig. 2) show, T1 and T2 were successfully conjugated to AgNPs as both T1-AgNP and T2-AgNP showed SPR band at 417 nm and 398 nm which is within the

expected SPR band range of 350 nm to 450 nm, indicating the formation of bonds between ligand (tetrazole) and AgNPs (Anwar et al. 2018). This study is focused on the development

**Fig. 6** Tetrazole-conjugated AgNPs and tetrazoles alone exhibited low host cell cytotoxicity. The assay was carried out by treating HeLa cells with 5 μM, 10 μM, 25 μM, and 50 μM of T1 and T2 respectively as well as 5 μM and 10 μM of tetrazole-conjugated AgNPs and AgNPs alone in RPMI-1640 followed by incubation for 24 h at 37 °C in a 5% CO<sub>2</sub> incubator. After the 24-h incubation period, the supernatant of each well was transferred to microcentrifuge tubes and lactate dehydrogenase enzyme (LDH) assay was carried out to determine % cytotoxicity



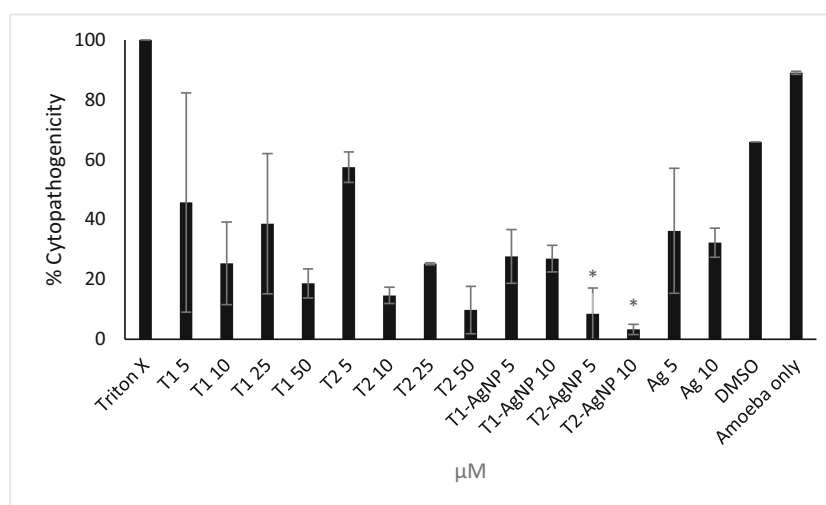


**Fig. 7** T2-conjugated AgNPs significantly decreased % cytopathogenicity of *A. castellanii*. This assay was carried out by treating  $5 \times 10^5$  *A. castellanii* trophozoites with 5 μM, 10 μM, 25 μM, and 50 μM of T1 and T2 respectively as well as 5 μM and 10 μM of tetrazole-conjugated AgNPs and AgNPs alone in RPMI-1640. After a 2-h

incubation period, the treated trophozoites were used to treat HeLa cells in 96-well plates at 37 °C for 24 h. After the 24-h incubation period, the supernatant of each well was transferred to microcentrifuge tubes and lactate dehydrogenase enzyme (LDH) assay was carried out to determine % cytopathogenicity

of anti-*A. castellanii* agent using two new synthetic tetrazoles and tetrazole-conjugated AgNPs. Antiamoebic assays showed (Figs. 3, 4, and 5) that at concentration 10 μM and above, T2 showed promising antiamoebic activities compared with T1 while encystation and excystation assays reveal that both T1 and T2 inhibited differentiation activity of *Acanthamoeba castellanii*. The use of T1 and T2 can allow the prevention of encystation of trophozoites, which makes the pathogen more susceptible to the antiamoebic effects of the tetrazoles or other drugs (Dart et al. 2009). Conjugation of T1 and T2 to AgNP also successfully increased the antiamoebic activities. This may be due to the increased bioavailability as AgNP allows better delivery of treatment compounds to *A. castellanii* by altering the shape, size, and surface properties of nanoparticles (Anwar et al. 2018). Host cell cytotoxicity and cytopathogenicity assays were also carried out to evaluate the host cell cytotoxicity as there is a lack of high-efficacy treatment with little adverse effects in treating AK and GAE. Cell cytotoxicity assay (Fig. 6) revealed that tetrazoles and AgNPs are significantly less toxic towards host cells compared with chlorhexidine which is known to cause undesirable side effects. Cytopathogenicity assay also revealed that T2-conjugated AgNPs reduced cytopathogenicity of *A. castellanii* compared with T2 alone (Fig. 7), suggesting that T2 is an effective anti-*Acanthamoeba* agent.

## Conclusion

In conclusion, the study suggests that T1- and T2-conjugated AgNPs are effective anti-*Acanthamoeba* agents with minimal adverse effects compared with chlorhexidine. This may be due

to the increased bioavailability as AgNP allows better delivery of treatment compounds to *A. castellanii*. Metal nanoparticles can potentially accumulate in the liver; therefore, the degradation process of nanoparticles should be addressed. It is crucial to further study the mechanism of pathogenesis of *Acanthamoeba* to better understand the crucial receptors that play a role in the process. This would ultimately lead to a more targeted and effective treatment for *Acanthamoeba* infections. However, animal studies should be performed to validate these results.

**Author's contributions** The study was conducted by team effort of all authors. The manuscript was submitted with the consent of all authors.

**Funding information** This work is supported by the Sunway University, Malaysia (GRTIN-RRO-98-2020), and the Pakistan Academy of Sciences for providing financial support Project No. (5-9/PAS/440).

## Compliance with ethical standards

**Conflict of interest** The authors declare that they have no conflict of interest.

**Ethical approval** Not required.

## References

- Anwar A, Siddiqui R, Hussain MA, Ahmed D, Shah MR, Khan NA (2018) Silver nanoparticle conjugation affects antiacanthamoebic activities of amphotericin B, nystatin, and fluconazole. *Parasitol Res* 117(1):265–271
- Anwar A, Khan NA, Siddiqui R (2019) Galactose as novel target against *Acanthamoeba* cysts. *PLoS Negl Trop Dis* 13(7):e0007385
- Anwar A, Ting ELS, Anwar A, Ul Ain N, Faizi S, Shah MR, Khan NA, Siddiqui R (2020) Antiamoebic activity of plant-based natural

- products and their conjugated silver nanoparticles against *Acanthamoeba castellanii* (ATCC 50492). *AMB Express* 10(1):24
- Aqeel Y, Siddiqui R, Anwar A, Shah MR, Khoja S, Khan NA (2015) Photochemotherapeutic strategy against *Acanthamoeba* infections. *Antimicrob Agents Chemother* 59(6):3031–3041
- Aqeel Y, Siddiqui R, Anwar A, Shah MR, Khan NA (2016) Gold nanoparticle conjugation enhances the antiacanthamoebic effects of chlorhexidine. *Antimicrob Agents Chemother* 60(3):1283–1288
- Band RN, Mohrlök S (1973) The cell cycle and induced amitosis in *Acanthamoeba*. *J Protozool* 20(5):654–657
- Barisani-Asenbauer T, Walochnik J, Mejdoubi L, Binder S (2012) Successful management of recurrent *Acanthamoeba* keratitis using topical and systemic miltefosine. *Acta Ophthalmol* 90:0–0
- Bello-Vieda N, Pastrana H, Garavito M, Ávila A, Celis A, Muñoz-Castro A, Restrepo S, Hurtado J (2018) Antibacterial activities of azole complexes combined with silver nanoparticles. *Molecules* 23(2):361
- Bendensky A, Menéndez D, Ostrosky-Wegman P (2002) Is metronidazole carcinogenic? *Mutat Res/Rev Mutat Res* 511(2):133–144
- Cabello-Vílchez AM, Martín-Navarro CM, López-Arencibia A, Reyes-Batlle M, Sifaoui I, Valladares B, Piñero JE, Lorenzo-Morales J (2014) Voriconazole as a first-line treatment against potentially pathogenic *Acanthamoeba* strains from Peru. *Parasitol Res* 113(2):755–759
- Cano PA, Islas-Jácome A, González-Marrero J, Yépez-Mulia L, Calzada F, Gámez-Montaño R (2014) Synthesis of 3-tetrazolylmethyl-4H-chromen-4-ones via Ugi-azide and biological evaluation against *Entamoeba histolytica*, *Giardia lamblia* and *Trichomona vaginalis*. *Bioorg Med Chem* 22(4):1370–1376
- Chopra A, Khuller GK (1983) Lipids of pathogenic fungi. *Prog Lipid Res* 22(3):189–220
- Dai LL, Zhang HZ, Nagarajan S, Rasheed S, Zhou CH (2015) Synthesis of tetrazole compounds as a novel type of potential antimicrobial agents and their synergistic effects with clinical drugs and interactions with calf thymus DNA. *MedChemComm* 6(1):147–154
- Dart JK, Saw VP, Kilvington S (2009) *Acanthamoeba* keratitis: diagnosis and treatment update 2009. *Am J Ophthalmol* 148(4):487–499
- Egger S, Lehmann RP, Height MJ, Loessner MJ, Schuppler M (2009) Antimicrobial properties of a novel silver-silica nanocomposite material. *Appl Environ Microbiol* 75(9):2973–2976
- Fatima I, Zafar H, Khan KM, Saad SM, Javaid S, Perveen S, Choudhary MI (2018) Synthesis, molecular docking and xanthine oxidase inhibitory activity of 5-aryl-1H-tetrazoles. *Bioorg Chem* 79:201–211
- Garajová M, Mrva M, Timko L, Lukáč M, Ondriska F (2014) Cytomorphological changes and susceptibility of clinical isolates of *Acanthamoeba* spp. to heterocyclic alkylphosphocholines. *Exp Parasitol* 145:S102–S110
- Garajová M, Mrva M, Vašková N, Martinka M, Melicherová J, Valigurová A (2019) Cellulose fibrils formation and organisation of cytoskeleton during encystment are essential for *Acanthamoeba* cyst wall architecture. *Sci Rep* 9(1):4466
- Gupta AK, Lyons DC (2015) The rise and fall of oral ketoconazole. *J Cutan Med Surg* 19(4):352–357
- Hitchcock CA, Dickinson K, Brown SB, Evans EGV, Adams DJ (1990) Interaction of azole antifungal antibiotics with cytochrome P-450-dependent 14 $\alpha$ -sterol demethylase purified from *Candida albicans*. *Biochem J* 266(2):475–480
- Khan NA (2006) *Acanthamoeba*: biology and increasing importance in human health. *FEMS Microbiol Rev* 30(4):564–595
- Khunkitti W, Lloyd DFJR, Furr JR, Russell AD (1998) *Acanthamoeba castellanii*: growth, encystment, excystment and biocide susceptibility. *J Inf Secur* 36(1):43–48
- Kim S, Kwon K, Kwon IC, Park K (2009) Nanotechnology in drug delivery: past, present, and future. In: *Nanotechnology in drug delivery*. Springer, New York, pp 581–596
- Köhler M, Mrva M, Walochnik J (2016) *Acanthamoeba*. In: *Molecular parasitology. Protozoan parasites and their molecules*. Springer-Verlag, Wien, pp 285–324
- Kulsoom H, Baig AM, Siddiqui R, Khan NA (2014) Combined drug therapy in the management of granulomatous amoebic encephalitis due to *Acanthamoeba* spp., and *Balamuthia mandrillaris*. *Exp Parasitol* 145:S115–S120
- Lamb DC, Warrilow AG, Rolley NJ, Parker JE, Nes WD, Smith SN, Kelly DE, Kelly SL (2015) Azole antifungal agents to treat the human pathogens *Acanthamoeba castellanii* and *Acanthamoeba polyphaga* through inhibition of sterol 14 $\alpha$ -demethylase (CYP51). *Antimicrob Agents Chemother* 59(8):4707–4713
- Lingling D, Shengfeng C, Damu GL, Chenghe Z (2013) Recent advances in the synthesis and application of tetrazoles. *Chinese J Org Chem* 33(2):224–244
- Lorenzo-Morales J, Khan NA, Walochnik J (2015) An update on *Acanthamoeba* keratitis: diagnosis, pathogenesis and treatment. *Parasite* 22:10
- Łukowska-Chojnacka E, Mierzejewska J, Milner-Krawczyk M, Bondaryk M, Staniszevska M (2016) Synthesis of novel tetrazole derivatives and evaluation of their antifungal activity. *Bioorg Med Chem* 24(22):6058–6065
- Nampoothiri RV, Malhotra P, Jain A, Batra N, Gupta K, Saj F, Khurana S, Mahalingam H, Lal A, Mukherjee K, Radotra B, Varma S (2018) An unusual cause of central nervous system infection during acute myeloid leukemia induction chemotherapy: *Acanthamoeba* brain abscess. *Indian J Hematol Blood Transfus* 34(1):153–155
- Padzik M, Hendiger EB, Chomicz L, Grodzik M, Szmidt M, Grobelny J, Lorenzo-Morales J (2018) Tannic acid-modified silver nanoparticles as a novel therapeutic agent against *Acanthamoeba*. *Parasitol Res* 117(11):3519–3525
- Padzik M, Hendiger EB, Żochowska A, Szczepaniak J, Baltaza W, Pietruczuk-Padzik A, Oleńska G, Chomicz L (2019) Evaluation of *in vitro* effect of selected contact lens solutions conjugated with nanoparticles in terms of preventive approach to public health risk generated by *Acanthamoeba* strains. *Ann Agric Environ Med* 26(1):198–202
- Parveen S, Misra R, Sahoo SK (2012) Nanoparticles: a boon to drug delivery, therapeutics, diagnostics and imaging. *Nanomed: Nanotechnol Biol Med* 8(2):147–166
- Schuster FL, Visvesvara GS (2004) Free-living amoebae as opportunistic and non-opportunistic pathogens of humans and animals. *Int J Parasitol* 34(9):1001–1027
- Sharma R, Jhanji V, Satpathy G, Sharma N, Khokhar S, Agarwal T (2013) Coinfection with *Acanthamoeba* and *Pseudomonas* in contact lens-associated keratitis. *Optom Vis Sci* 90(2):e53–e55
- Siddiqui R, Khan NA (2012) Biology and pathogenesis of *Acanthamoeba*. *Parasit Vectors* 5(1):6
- Sissons J, Alsam S, Stins M, Rivas AO, Morales JL, Faull J, Khan NA (2006) Use of *in vitro* assays to determine effects of human serum on biological characteristics of *Acanthamoeba castellanii*. *J Clin Microbiol* 44(7):2595–2600
- Slater CA, Sickel JZ, Visvesvara GS, Pabico RC, Gaspari AA (1994) Successful treatment of disseminated *Acanthamoeba* infection in an immunocompromised patient. *N Engl J Med* 331(2):85–87
- Tavassoli S, Buckle M, Tole D, Chiodini P, Darcy K (2018) The use of miltefosine in the management of refractory *Acanthamoeba* keratitis. *Contact Lens Anterior Eye* 41(4):400–402
- Timko L, Fischer-Fodor E, Garajová M, Mrva M, Chereches G, Ondriska F, Bukovský M, Lukáč M, Karlovská J, Kubincová J, Devínsky F (2015) Synthesis of structural analogues of hexadecylphosphocholine and their antineoplastic, antimicrobial and amoebicidal activity. *Eur J Med Chem* 93:263–273
- Tu EY, Joslin CE, Shoff ME (2010) Successful treatment of chronic stromal *Acanthamoeba* keratitis with oral voriconazole monotherapy. *Cornea* 29(9):1066
- Webster D, Umar I, Kolyvas G, Bilbao J, Guiot MC, Duplisea K, Qvarnstrom Y, Visvesvara GS (2012) Treatment of granulomatous amoebic encephalitis with voriconazole and miltefosine in an immunocompetent soldier. *Am J Trop Med Hyg* 87(4):715–718

- Weisman RA (1976) Differentiation in *Acanthamoeba castellanii*. Annu Rev Microbiol 30(1):189–219
- Xuguang S, Lin C, Yan Z, Zhiqun W, Ran L, Shiyun L, Xiuying J (2003) *Acanthamoeba* keratitis as a complication of orthokeratology. Am J Ophthalmol 136(6):1159–1161
- Zazo H, Colino CI, Lanao JM (2016) Current applications of nanoparticles in infectious diseases. J Control Release 224:86–102

**Publisher's note** Springer Nature remains neutral with regard to jurisdictional claims in published maps and institutional affiliations.